



ELSEVIER

Available online at www.sciencedirect.com

SCIENCE @ DIRECT®

Journal of Magnetism and Magnetic Materials 266 (2003) 96–101

Journal of
magnetism
and
magnetic
materials

www.elsevier.com/locate/jmmm

Oxidation of FePt nanoparticles

Chao Liu^{a,*}, Timothy J. Klemmer^a, Nisha Shukla^a, Xiaowei Wu^a, Dieter Weller^a,
Mihaela Tanase^b, David Laughlin^b

^a *Seagate Research, 1251 Waterfront Place, Pittsburgh, PA 15222, USA*

^b *Data Storage Systems Center, Carnegie Mellon University, Pittsburgh, PA 15213, USA*

Received 20 November 2002

Abstract

Chemically disordered ~ 3 – 7 -nm-diameter FePt nanoparticles are synthesized using the airless operation technique based on decomposition of iron pentacarbonyl and reduction of platinum acetylacetonate. The particle solution is then washed and subsequently deposited onto a thermally oxidized Si substrate. Nanoparticle assemblies are formed after solvent evaporation. The samples are heat-treated using rapid thermal annealing at 650°C for 30 min, in an atmosphere of Ar gas with less than 1 ppm of O_2 . Oxidation has to be avoided to obtain the FePt L_{10} phase. Other crystalline phases such as FePt_3 (L_{12}), magnetite Fe_3O_4 , hematite Fe_2O_3 and FCC Pt are obtained if oxygen is present.

© 2003 Elsevier B.V. All rights reserved.

Keywords: L_{10} Phase; FePt; Magnetic nanoparticles; Oxidation; Phase transformation

1. Introduction

Nanometer-scale materials with novel properties have attracted extensive research in a variety of fields [1–7]. Magnetic nanoparticles, for example, exhibit size effects [8–10]. Below a critical size, magnetic nanoparticles comprise single domains, in contrast to respective bulk materials, which typically have multiple domains. Magnetic nanoparticles show interesting phenomena such as superparamagnetism and quantum tunneling of magnetization. Because of the unique properties, magnetic nanoparticles have great potential for applications in diverse areas such as magnetic refrigeration [11], cell separation and magnetically

guided drug delivery [12–14], magnetic resonance imaging (MRI) contrast enhancement [15], ferrofluids [16] and magnetic recording [17–20]. Colloidal chemistry synthesis and self-assembly procedures demonstrate great promise in making monodispersed magnetic nanoparticles and large area arrays. Fabrication of respective nanostructures with control over size, size distribution, crystalline phase and chemical composition, however, remains a major challenge. The first successful demonstration of monodispersed FePt nanoparticle structures has been accomplished recently based on solution-phase chemical synthesis [20]. Annealing is required to induce a phase transformation from the low-anisotropy face-centered cubic (FCC), chemically disordered phase to the high-anisotropy chemically ordered L_{10} phase. However, it is interesting to study the

*Corresponding author.

E-mail address: chao.liu@seagate.com (C. Liu).

annealing reaction in the presence of oxygen to further understand the role of oxidation of the nanoparticles. It is not clear what the size effect of the nanoparticles on the oxidation reactions would be. In order to study the effect of oxygen on the nanoparticles a first step would be to drive the oxidation reaction to extreme conditions and compare to known bulk oxidation conditions.

2. Experimental

Chemically disordered FePt nanoparticles are synthesized using Sun's approach based on decomposition of iron pentacarbonyl and reduction of platinum acetylacetonate. The particle solution is then washed and subsequently deposited onto a thermally oxidized Si substrate. Nanoparticle assemblies are formed after solvent evaporation. Phase transformation from as-prepared chemically disordered FCC phase to chemically ordered $L1_0$ phase is achieved by heat treatment using rapid thermal annealing. Oxidation studies are done by using conventional oven anneal with different oxygen levels.

Transmission electron microscope (TEM) samples are prepared by depositing a drop of dilute FePt nanoparticle solution onto a carbon-coated copper grid. The studies are done using a Philips TECNAI transmission electron microscope operating at 200 kV. XRD studies on the as-prepared samples and annealed samples are done using a Philips X'PERT PRO MRD equipped with an X-ray mirror using primarily asymmetric glancing incidence scans with the incident angle set at 3° .

3. Results and discussions

The chemical composition of FePt nanoparticles can be adjusted by controlling the molar ratio of iron carbonyl to the platinum salt. However, the reaction temperature for decomposition of iron pentacarbonyl and reduction of platinum acetylacetonate is higher than the boiling point of iron pentacarbonyl, which is 103°C . Only part of the iron from the pentacarbonyl is incorporated into the particles with the excess being lost. In addition,

there are some concerns about the possible core/shell structure and inhomogeneous distribution of Fe and Pt [21] since the reaction mechanisms and nucleation mechanisms are not completely clear yet. It has been suggested that iron pentacarbonyl is actually in the vapor phase, which results in the slow decomposition of iron pentacarbonyl at a rate that matches the reduction rate of platinum acetylacetonate [18–19]. HRTEM image for an as-prepared sample is shown in Figs. 1(a) and (b) and demonstrates a faceted morphology that has been studied in detail by Wang et al. [22]. The average diameter of these as-prepared nanoparticles is 4.48 nm with a standard deviation of 0.15 nm.

These nanoparticles are regarded as monodispersed and they self-assemble into an organized assembly when deposited under the right conditions. Fig. 1(c) shows that no ordered superlattice peaks are present in an XRD $\theta-2\theta$ scan, which is characteristic for the chemically disordered FePt alloy with FCC phase. Separate peaks for Fe and Pt are not present providing evidence of an FCC alloy of Fe and Pt. Additionally, the uniform lattice across the particles from high-resolution TEM image demonstrates that the particles are homogeneous (a core structure of Fe and Pt is not observed) with respect to the elemental distribution of Fe and Pt, which means that during the chemical synthesis Fe and Pt are distributed randomly on the FCC lattice. Also in the XRD scan an amorphous carbon peak resulting from the surfactant that is applied to avoid the agglomerations of the particles is observed. The random crystallographic orientation of the particles is evident from the intensity ratios of the indexed peaks in the XRD scan being approximately equal to those from powder diffraction files.

The phase transformation from as-prepared chemically disordered to chemically ordered $L1_0$ phase can be achieved by the heat treatment using rapid thermal annealing at a relatively high temperature of 650°C for 30 min in an atmosphere of Ar gas with less than 1 ppm of O_2 . Annealing at 650°C for 30 min should drive the chemically disorder-order phase transformation into equilibrium. The chemically ordered $L1_0$ phase is verified by the XRD pattern in Fig. 2 and the electron diffraction pattern (inset of Fig. 2). In

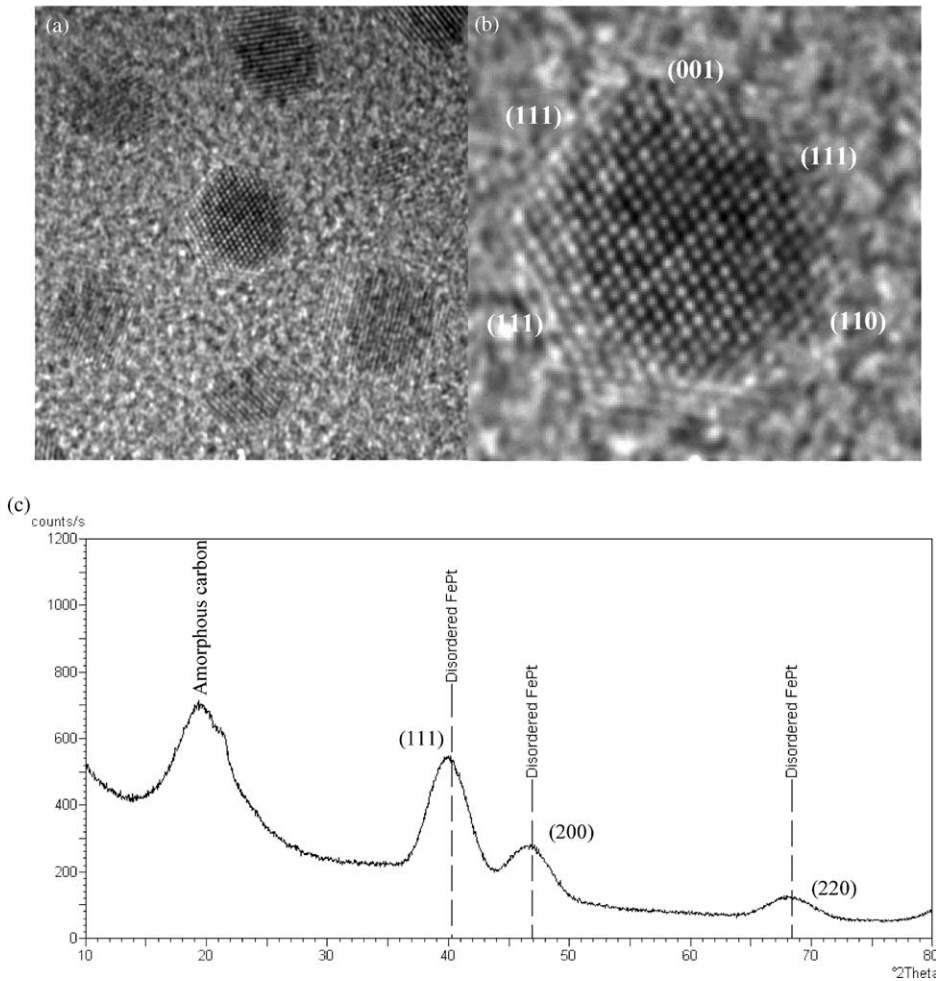


Fig. 1. (a) HRTEM image of as-prepared FePt nanoparticles. An enlarged HRTEM image of one individual FePt particle is shown in (b). (c) X-ray diffraction pattern of as-prepared FePt nanoparticles.

order to measure the lattice parameters (both c and a), the superlattice peaks of (001) and (110) were fitted and used to calculate the c - and a -parameter, respectively. Additionally the (200)/(002) peak was de-convoluted and also used to calculate c and a lattice parameters. Profile fitting of the X-ray diffraction pattern revealed that the lattice constant a is 3.86 Å and c is 3.72 Å, with c/a ratio being 0.964. This is quite consistent with the lattice constant for near-equiatomic FePt bulk material with $L1_0$ phase [23].

However, if the particles are annealed in the presence of oxygen, oxidation of the particles is

possible. Although Pt is a noble metal and therefore Pt oxides are not stable, Fe has the potential for oxidation into three different oxides: wustite (FeO), magnetite (Fe₃O₄), and hematite (Fe₂O₃). Wustite is FCC, can exist over a broad range of stoichiometry and is only stable at temperatures > 570°C. Magnetite and hematite are inverse spinel and rhombohedral structures, respectively, and both are almost stoichiometric at temperatures below ~1000°C. For bulk materials at atmospheric conditions it is known that hematite is the most thermodynamically stable followed by magnetite and finally wustite.

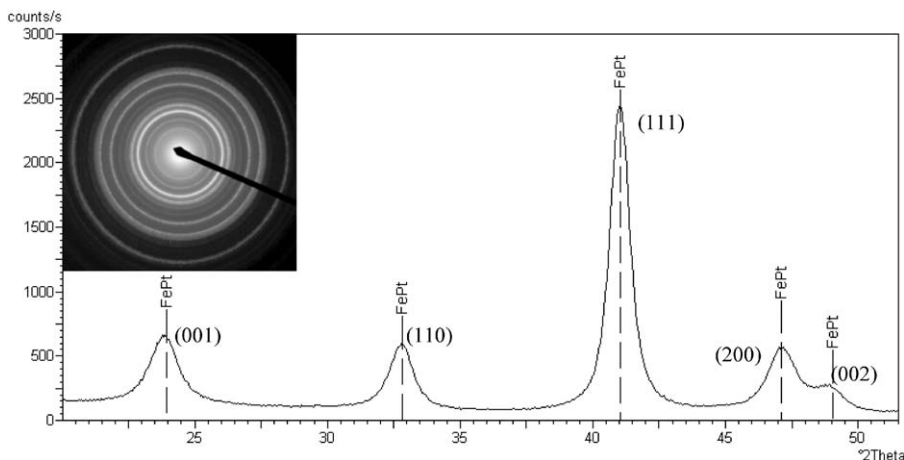


Fig. 2. X-ray diffraction pattern of annealed FePt nanoparticles after annealing at 650°C for 30 min by RTP.

Fig. 3a shows a FePt nanoparticle sample of similar Fe–Pt concentration as the sample shown in Fig. 2, but annealed at 700°C for 30 min in the presence of oxygen. The XRD scan reveals a two-phase mixture of Fe₃O₄ and an FePt ordered alloy. It is clear that the alloy is ordered because of the superlattice reflections, which are observed. In the absence of the oxide, the alloy composition was near the 50% Fe composition; however, some of the Fe is now tied up in the oxide and therefore the metal alloy composition is now depleted into Fe. From the position of the superlattice peaks (001) and (110), the position of the (111) fundamental and the fact that the (200) has not split, it can be concluded that the ordered phase is near the L₁₂ FePt₃ phase in composition. Apparently, the annealing causes the oxidation while at the same time allowing the remaining Fe and Pt to chemically order in the equilibrium phase for the composition of the alloy. The peak positions are shifted a little bit to lower angles in the XRD pattern relative to the standard diffraction peaks of FePt₃ with L₁₂ phase. Even though Vegard's law is not strictly obeyed by metallic solid solutions, it is often used as a sort of yardstick by which one solution may be compared with another. We have previously demonstrated that a shift in peak position can be used to monitor the relative chemical composition of the FePt alloy [24]. This shift in peak position is consistent with

Vegard's law which states that the lattice parameter of a binary solid solution is proportional to the atomic percent of the alloy. These shifted peaks can be ascribed to the Fe_{1-x}Pt_{3+x} alloy with 0 < x < 1, which consists of less Fe atoms in solid solution than FePt₃. If a macroscopic EDAX measurement was made on a sample where some of the Fe is tied up with oxygen and the Fe/Pt ratio was measured, the composition would come out as stoichiometric but the sample would show poor magnetism because the alloy is not in the L₁₀ phase. Magnetic hysteresis results of the oxidized samples show that the coercivity is almost zero at room temperature. The sample with L₁₀ phase shown in Fig. 2 has a coercivity of 14.7 kOe at room temperature. The low coercivity of the oxidized samples is consistent with the low magnetocrystalline anisotropy of the ferrimagnetic magnetite. The FePt₃ with L₁₂ structure is typically antiferromagnetic and hematite is diamagnetic at room temperature and therefore does not contribute to the magnetic hysteresis.

It is also interesting to note that wustite is not present. The reason for this may be because the annealing temperature is only ~130°C above its stable temperature; therefore, the driving force for the formation of this oxide is small and results in a large activation energy for nucleation. Additionally, wustite is often observed in bulk materials when a continuous oxide causes a gradient of

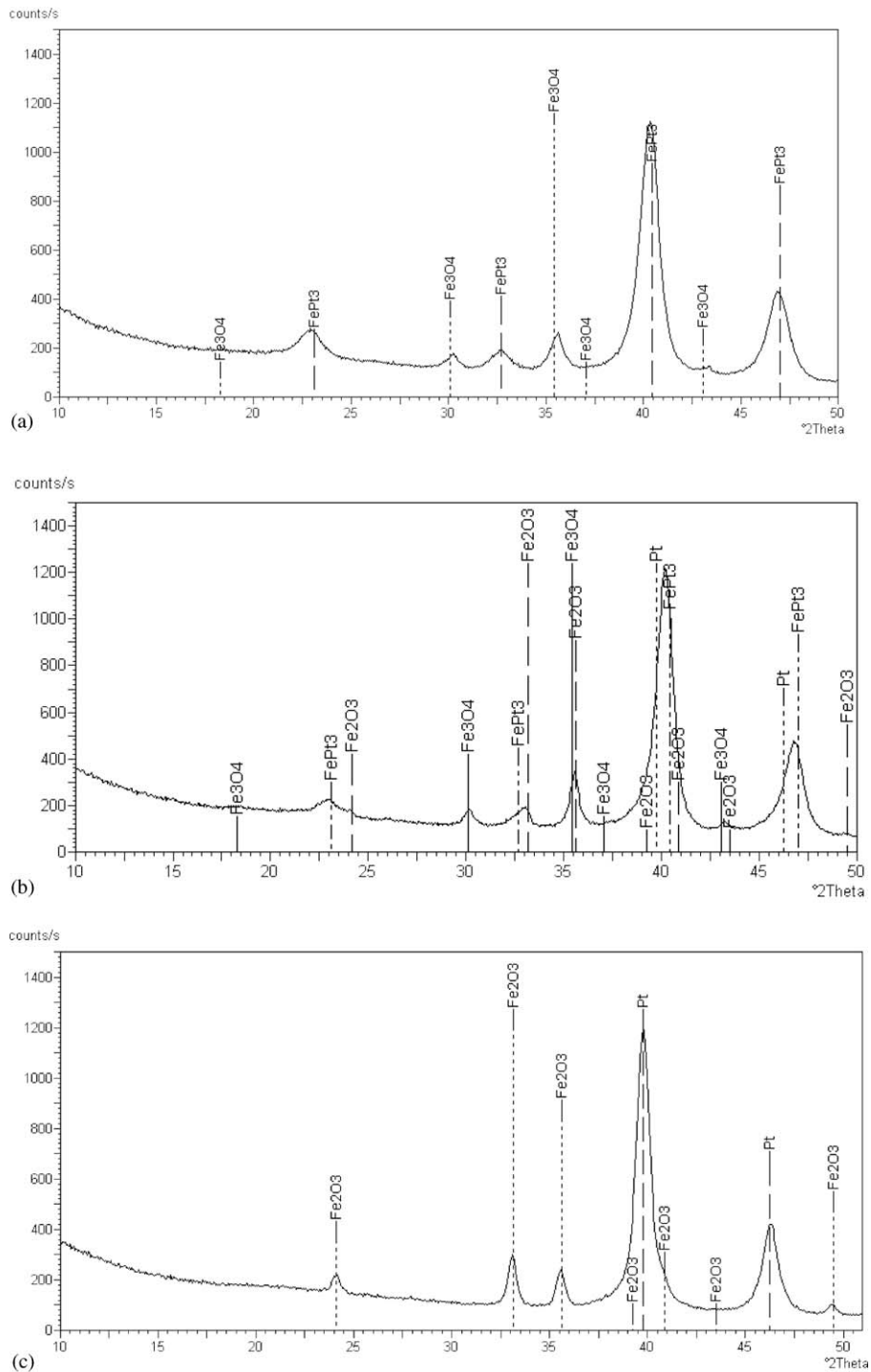


Fig. 3. X-ray diffraction pattern for the samples obtained through heat treatment in the presence of oxygen. Both $L1_2$ FePt_3 and magnetite Fe_3O_4 crystalline phases are indicated for sample (a). Sample (c) is composed of pure Pt with FCC phase and hematite Fe_2O_3 . Crystalline phases for sample (b) include hematite Fe_2O_3 , magnetite Fe_3O_4 , and Fe_xPt_3 alloy with $0 < x < 1$.

oxygen with depth from the surface. It is not clear that the oxides of our nanoparticles are continuous. With an additional anneal of 600°C for 30 min the XRD pattern shown in Fig. 3b is observed. Here we observe a three-phase mixture of Fe₃O₄, Fe₂O₃ and FePt ordered alloys (near FePt₃ composition). This results because the oxygen has diffused further into the material causing the concentration of oxygen to increase, thereby producing Fe₂O₃. When a similar sample is annealed at 700°C for 30 min but in a higher partial pressure of oxygen XRD pattern shown in Fig. 3c is obtained. The result is a two-phase mixture of Fe₂O₃ and Pt. The superlattice reflections have disappeared as expected for a pure metal. Here, the oxidation has been driven to equilibrium where the most stable Fe oxide and the noble metal Pt is all that is left.

4. Conclusion

Monodispersed FePt nanoparticles are synthesized based on decomposition of iron pentacarbonyl and reduction of platinum acetylacetonate. Heat-treatment conditions on phase transformation of the FePt nanoparticles from as-prepared chemically disordered FCC phase to chemically ordered phases are studied. Chemically ordered L1₀ FePt particles are obtained after annealing at 650°C for 30 min, in an atmosphere of Ar gas with less than 1 ppm of O₂. When annealing in the presence of oxygen other crystalline phases such as oxides including magnetite Fe₃O₄ and hematite Fe₂O₃ can form with metals of varying Fe contents depending on how far the oxidation reaction is driven to equilibrium. Therefore, oxidation may be a problem for annealing FePt nanoparticles of stoichiometric composition to produce the ordered L1₀ phase.

References

- [1] Clusters (special issue), *Science*, 271 (1996).
- [2] Nanostructured materials (special issue), *Chem. Mater.* 8 (1996).
- [3] T.S. Ahmadi, Z.L. Wang, T.C. Green, A. Henglein, M.A. El-Sayed, *Science* 28 (1996) 1924.
- [4] C. Liu, B. Zou, A.J. Rondinone, Z.J. Zhang, *J. Am. Chem. Soc.* 123 (2001) 4344.
- [5] C.B. Murray, C.R. Kagan, M.G. Bawendi, *Science* 270 (1995) 1335.
- [6] C. Liu, B. Zou, A.J. Rondinone, Z.J. Zhang, *J. Am. Chem. Soc.* 122 (26) (2000) 6263.
- [7] S. O'Brien, L. Brus, C.B. Murray, *J. Am. Chem. Soc.* 123 (2001) 12085.
- [8] Z.X. Tang, J.P. Chen, C.M. Sorensen, K.J. Klabunde, G.C. Hadjipanayis, *Phys. Rev. Lett.* 68 (1992) 3114.
- [9] P.J. Van der Zaag, A. Noordermeer, M.T. Johnson, P.F. Bongers, *Phys. Rev. Lett.* 68 (1992) 3112.
- [10] C. Liu, Z.J. Zhang, *Chem. Mater.* 13 (2001) 2092.
- [11] K.A. Gschneider Jr., V.K. Pecharsky, *J. Appl. Phys.* 85 (1999) 5365.
- [12] Marcel De Cuyper, Marcel Joniau, *J. Magn. Magn. Mater.* 122 (1993) 340.
- [13] E.K. Ruuge, A.N. Rusetski, *J. Magn. Magn. Mater.* 122 (1993) 335.
- [14] U. Häfeli, W. Schütt, J. Teller, M. Zborowski, *Scientific and Clinical Applications of Magnetic Carriers*, Plenum, New York, 1997.
- [15] D.G. Mitchell, *J. Magn. Reson. Imaging* 7 (1997) 1.
- [16] K. Raj, R. Moskowitz, *J. Magn. Magn. Mater.* 85 (1990) 233.
- [17] M.H. Kryder, *MRS Bull.* 21 (1996) 17.
- [18] S. Sun, D. Weller, *J. Magn. Soc. Japan* 25 (2001) 1434.
- [19] S. Sun, E.E. Fullerton, D. Weller, C.B. Murray, *IEEE Trans. Magn.* 37 (2001) 1239.
- [20] S. Sun, C.B. Murray, D. Weller, L. Folks, A. Moser, *Science* 287 (2000) 1989.
- [21] J. Park, J. Cheon, *J. Am. Chem. Soc.* 123 (2001) 5743.
- [22] Z.R. Dai, S. Sun, Z.L. Wang, *Surf. Sci.* 505 (2002) 325.
- [23] JCPDS-International Centre for Diffraction Data, 1999.
- [24] T.J. Klemmer, N. Shukla, C. Liu, X.W. Wu, E.B. Svedberg, O. Mryasov, R.W. Chantrell, D. Weller, M. Tanase, D.E. Laughlin, *Appl. Phys. Lett.* 81 (2002) 2220.